Molecular Therapy
Nucleic Acids
Original Article

Limiting Thymic Precursor Supply Increases the Risk of Lymphoid Malignancy in Murine X-Linked Severe Combined Immunodeficiency

Samantha L. Ginn,[1] Claus V. Hallwirth,[1] Sophia H.Y. Liao,[1] Erdahl T. Teber,[2] Jonathan W. Arthur,[2] Jianmin Wu,[3,4,11] Hong Ching Lee,[3,4] Szun S. Tay,[1] Min Hu,[5] Roger R. Reddel,[6] Matthew P. McCormack,[7] Adrian J. Thrasher,[8] Marina Cavazzana,[9] Stephen I. Alexander,[5,10] and Ian E. Alexander[1,10]

[1]Gene Therapy Research Unit, Children's Medical Research Institute, The University of Sydney and The Sydney Children's Hospitals Network, Westmead, NSW 2145, Australia; [2]Bioinformatics Unit, Children's Medical Research Institute, The University of Sydney, Westmead, NSW 2145, Australia; [3]Kinghorn Cancer Centre & Cancer Division, Garvan Institute of Medical Research, Darlinghurst, NSW 2010, Australia; [4]St Vincent's Clinical School, University of New South Wales, Darlinghurst, NSW 2010, Australia; [5]Centre for Kidney Research of The Children's Hospital at Westmead, Westmead, NSW 2145, Australia; [6]Cancer Research Unit, Children's Medical Research Institute, The University of Sydney, Westmead, NSW 2145, Australia; [7]Australian Centre for Blood Diseases, Monash University, Melbourne, VIC 3800, Australia; [8]Infection, Immunity, Inflammation, UCL Great Ormond Street Institute of Child Health, London WC1N 1EH, UK; [9]Department of Biotherapy, Hôpital Necker-Enfants Malades, Paris 75015, France; [10]Discipline of Child and Adolescent Health, The University of Sydney, Westmead, NSW 2145, Australia

In early gene therapy trials for SCID-X1, using γ-retroviral vectors, T cell leukemias developed in a subset of patients secondary to insertional proto-oncogene activation. In contrast, we have reported development of T cell leukemias in SCID-X1 mice following lentivirus-mediated gene therapy independent of insertional mutagenesis. A distinguishing feature in our study was that only a proportion of transplanted γc-deficient progenitors were transduced and therefore competent for reconstitution. We hypothesized that reconstitution of SCID-X1 mice with limiting numbers of hematopoietic progenitors might be a risk factor for lymphoid malignancy. To test this hypothesis, in the absence of transduction, SCID-X1 mice were reconstituted with serially fewer wild-type hematopoietic progenitors. A robust inverse correlation between hematopoietic progenitor cell dose and T-lymphoid malignancy was observed, with earlier disease onset at lower cell doses. Malignancies were of donor origin and carried activating *Notch1* mutations. These findings align with emerging evidence that thymocyte self-renewal induced by progenitor deprivation carries an oncogenic risk that is modulated by intra-thymic competition from differentiation-committed cells. Although insertional proto-oncogene activation is required for the development of malignancy in humans, failure of γc-deficient thymocytes to effectively compete with this at-risk cell population may have also contributed to oncogenesis observed in early SCID-X1 trials.

INTRODUCTION

Gene therapy for X-linked severe combined immunodeficiency (SCID-X1) has been successfully employed in the clinic by restoration of γc expression in bone-marrow-derived $CD34^+$ cells using integrating vectors.[1,2] In the earliest studies, using conventional γ-retroviral vectors, robust immune reconstitution was observed in the majority of infants, likely owing to the selective advantage of the transduced progenitors. However, despite successful phenotypic correction, 25% of treated infants developed T cell acute lymphoblastic leukemia (T-ALL) as a consequence of insertional mutagenesis. Furthermore, patients acquired secondary genomic abnormalities including activating mutations in *NOTCH1*.[3,4] Although the role of insertional mutagenesis via the activation of proto-oncogenes such as *LMO2* has been clearly implicated in the development of T-ALL in SCID-X1 patients following gene therapy, the absence of adverse events in patients treated similarly for adenosine deaminase deficiency (ADA-SCID), despite also exhibiting integrations near these proto-oncogenes, remains incompletely understood.

We have previously developed a mouse model of lentivirus-mediated correction of SCID-X1 and observed lymphoid malignancies.[5] Crucially, the oncogenic events observed in mice receiving gene therapy were not attributable to insertional mutagenesis, suggesting alternative mechanisms for genotoxic risk in this model. One significant difference between positive control SCID-X1 mice reconstituted with wild-type hematopoietic progenitor cells and SCID-X1 mice receiving gene therapy with an equivalent number of vector-exposed γc-deficient progenitor cells was the absolute number of cells received that were competent for lymphoid reconstitution. The gene therapy

Received 16 November 2016; accepted 21 November 2016;
http://dx.doi.org/10.1016/j.omtn.2016.11.011.

[11]Present address: Key Laboratory of Carcinogenesis and Translational Research (Ministry of Education/Beijing), Centre for Cancer Bioinformatics, Peking University Cancer Hospital & Institute, 52 Fu Cheng Road, Hai Dian District, Beijing 100142, China.

Correspondence: Professor Ian E. Alexander, Gene Therapy Research Unit, The Children's Hospital at Westmead, Locked Bag 4001, Westmead, NSW 2145, Australia.
E-mail: ian.alexander@health.nsw.gov.au

group received a lower dose on account of only a subset of vector-exposed γc-deficient cells being transduced. We therefore hypothesized that reconstitution of SCID-X1 mice with limiting numbers of hematopoietic progenitor cells might be a risk factor for lymphoid malignancy.

In the current study, we sought to explore the relationship between hematopoietic progenitor cell dose and the incidence of lymphoid malignancy by transplanting sub-lethally irradiated $\gamma c^{-/-}Rag^{-/-}$ mice with serially fewer wild-type $Sca1^{+}$ progenitor cells, in the absence of gene transfer. The progenitor cell doses examined fell within a range that supported immunological reconstitution, and the resultant lymphoid compartment sizes varied by no more than ~2-fold, despite up to 100-fold differences in hematopoietic progenitor cell dose. Of greatest interest, however, was the observation of a robust inverse correlation between cell dose and the incidence of T-lymphoid malignancy, with progressively shorter disease latency at lower cell doses. All malignancies were wild-type donor cell-derived and carried activating *Notch1* mutations.

Replicative stress has been implicated in the development of B cell leukemia in mice[6] and is a plausible antecedent to T-lymphoid oncogenesis in the current study. While encompassing this possibility, our findings fall within a conceptual framework provided by recent insights into murine thymocyte biology. Most notable among these is the observation of sustained thymic output despite complete T cell progenitor deprivation (thymus autonomy), with autonomous T cell production being supported by induction of a thymocyte self-renewal phenotype.[7–10] This self-renewal phenotype, which arises in the double-negative (DN) 3 thymic niche and can also be induced by deliberate *Lmo2* overexpression,[11] appears to carry an inherent risk of oncogenesis that is dependent upon acquisition of additional genetic lesions, such as *Notch1* mutations. Moreover, competition from bone-marrow-derived progenitors has been shown to increase the turnover of thymocytes with a self-renewal phenotype, thereby reducing the probability of acquiring oncogenic mutations.[10] Directly relevant to the SCID-X1 phenotype is the inability of γc-deficient thymic progenitors to progress to the DN3 niche, thereby reducing their ability to provide competition to γc-proficient progenitors.[9] Thus, data generated in our model are consistent with limiting thymic precursor supply, not only inducing a self-renewal phenotype in the murine thymus, but also simultaneously reducing competition in the DN3 niche with a resultant cell dose-dependent increase in oncogenic risk.

There is currently no evidence that limiting thymic precursor supply is a risk factor for lymphoid malignancy in humans; nevertheless, the possibility of cell competition acting as a tumor suppressor mechanism in the human thymus following vector-mediated insertional oncogene activation remains a compelling hypothesis. Coupled with disease-specific differences in the progression of thymic precursors through T cell ontogeny, this hypothesis has the potential to help explain differing risks of oncogenesis.

RESULTS

The Frequency of Lymphoid Malignancy Is Inversely Proportional to the Wild-Type Progenitor Cell Dose Used to Reconstitute SCID-X1 Mice

To explore the notion that limiting thymic precursor supply is a risk factor for oncogenesis, sub-lethally irradiated $\gamma c^{-/-}Rag2^{-/-}$ recipients were reconstituted with different doses of wild-type bone marrow hematopoietic progenitor cells (Figure 1A). We chose to use $\gamma c^{-/-}Rag2^{-/-}$ recipients because $IL2RG^{-/-}$ mice have been shown to have a "leaky" T cell phenotype that manifests with age[12] and would therefore not be suitable for longitudinal studies. Importantly, however, the donor cells were $IL2RG^{-/-}$. To ensure all mice received an equivalent cell dose, the total cell number was fixed at 5×10^5 per recipient animal, and, at the lower cell doses, $Sca1^{+}$ progenitor cells from $IL2RG^{-/-}$ mice (γc null) were combined with those expressing γc; 5×10^5 (high dose), 5×10^4 (mid dose) or 5×10^3 (low dose), with the latter two doses representing a phenocopy of 10% and 1% gene transfer, respectively. In this model, only wild-type cells are capable of progressing past the double-negative 2 (DN2) stage of thymic development.

To investigate long-term oncogenic risk, mice reconstituted with a high, mid, or low dose of γc-expressing progenitors were observed for up to 18 months. Lymphoid malignancies were never observed in mice receiving the high dose, consistent with our previous study[5] but detected exclusively in animals from the mid- and low-dose groups between 6.6 and 17.6 months post-transplantation (Figure 1B). The latency for oncogenesis was also significantly longer in the mid-dose group compared with low-dose group (12.8 ± 3.5 and 8.9 ± 1.4 months, respectively; $p = 0.02$). Of the 31 mice that had received the mid cell dose, four developed malignancy, while the incidence of malignancy was not significantly greater than in mice transplanted with the high dose of progenitors, the survival rate was decreased ($p = 0.03$). In the low-dose group, both the incidence of malignancy and malignancy-free survival rates were significantly different when compared with the high-dose group ($p = 0.0017$ and $p = 0.0001$, respectively). Of interest, the rate of malignancy in mice transplanted with the low dose of γc-expressing cells (33.3%) was similar to that observed in our previous study (28.6%).[5]

Phenotypic Characterization of Leukemic Clones

Necropsy showed hepatosplenomegaly with extensive blast infiltration, and histological analysis revealed marked disruption of tissue architecture in the liver, spleen, thymus (Figure 1C), lung, and kidney (data not shown). Interestingly, enlarged thymi containing malignant cells were almost exclusively present in mice transplanted with the lowest dose of γc-expressing progenitors, which was in contrast to mice that developed malignancy from the mid dose group, where the thymus was small or, in most cases, not macroscopically visible (Table 1).

Abnormal T cell populations in 12 of the 14 mice that developed malignancy were identified in the spleen, liver, thymus, bone marrow,

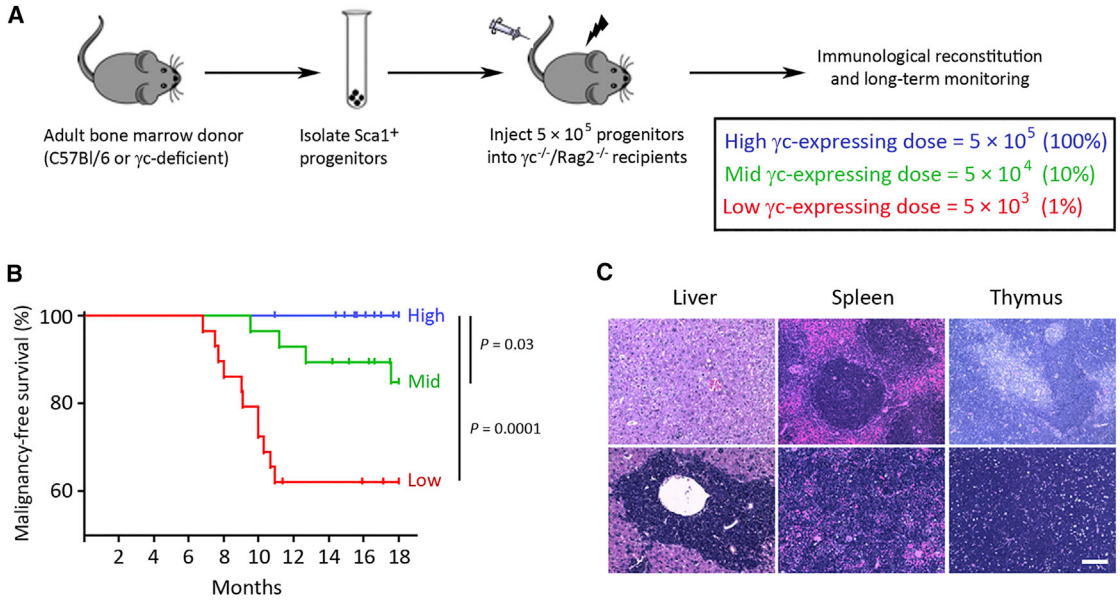

Figure 1. Incidence and Latency of Lymphoid Malignancies Observed under Conditions of Limiting Bone Marrow Progenitor Supply

(A) Experimental design. (B) Kaplan-Meier survival analysis at 18 months post-transplantation; animals receiving high, mid, and low wild-type γc-expressing cell doses are indicated in blue, green, and red, respectively. (C) H&E staining of C57BL/6 control (top panels) or malignant samples from an animal receiving the low-dose of γc-expressing progenitors (bottom panels, m209). Scale bar, 100 μm.

and peripheral blood. White blood cell counts were also elevated in these animals. The phenotypes of these tumors were diverse, with cells expressing immature, mature, and atypical combinations of surface markers (Table 1). In addition, two of the 14 malignancies (14.3%) did not express the T cell markers CD3, CD4, or CD8 and were B220 positive (m249 and m250).

Limiting Thymic Precursor Supply Did Not Prevent Reconstitution of the Immunological Compartment

Peripheral blood assessed at 6 (data not shown) and 16 weeks post-transplantation (Figure 2A) demonstrated lymphoid reconstitution with all three doses, with T, B, and natural killer (NK) cell compartments observed at the expected ratios. Lymphoid reconstitution for mice receiving the mid dose of γc-expressing cells was only approximately half (47%) that of animals receiving the high cell dose, despite receiving 10-fold fewer γc-expressing cells. For mice receiving the lowest dose of γc-expressing cells, lymphoid reconstitution was comparable to that of mice receiving the mid dose, and when compared to mice receiving the high dose of wild-type cells (i.e., 100-fold more γc-expressing cells), the lymphoid compartment was reduced to only 43%.

The level of bone marrow chimerism in mice reconstituted with either the high or low dose of wild-type (CD45.1 positive) progenitors was determined by flow cytometry. The contribution of wild-type cells was found to be 64.9% ± 3.0% (n = 8) in the high-dose group, indicating that the majority of cells engrafted in the bone marrow were derived from the wild-type γc-expressing progenitors. For animals transplanted with the low dose of wild-type cells, the contribution was 3.4% ± 0.3% (n = 7), consistent with only 1% of the transplanted cells expressing γc.

T Cell Receptor Diversity Is Maintained under Conditions of Limiting Thymic Precursor Supply

To determine whether T cell receptor (TCR) diversity was affected by limiting thymic precursor supply, TCR V_β repertoire and spectratype analyses (on selected highly expressed TCR V_β families) were performed at 15 weeks post-transplantation. Analysis of the TCR V_β repertoire demonstrated that, for the majority of cases, both broad representation of all V_β families and the percentage of each V_β family was equivalent in peripheral blood samples taken from mice receiving each of the three γc-expressing progenitor cell doses (Figure 2B). Spectratype analysis revealed normal Gaussian distribution of peaks in mice receiving the high and mid dose of γc-expressing progenitors for the majority of TCR V_β families investigated (Figure 2C). For mice reconstituted with low cell numbers, the spectratypes appeared more restricted for some TCR V_β families. The observation of a relatively diverse TCR V_β repertoire for all cohorts is suggestive of increased expansion of immature T cells at the low compared with the high cell dose prior to TCRβ rearrangement.

To assess the level of thymic T cell export occurring in vivo, the number of signal joint T cell receptor excision circles (sjTRECs), a by-product of TCRα rearrangement, was quantified in sorted splenic T cell populations at 16 weeks post-transplantation (Figure 2D). The numbers of sjTRECs isolated from mice receiving the high and mid doses were similar, implying that the transplanted cells had undergone comparable cell division after TCRα rearrangement, which

Table 1. Latency and Cellular Immunophenotype of Lymphoid Malignancies

Wild-Type Cell Dose	Mouse	Latency (Months)	Immunophenotype	Thymus Weight (g)[a]
5×10^4	50	12.7	$CD3^+$ $CD4^-$ $CD8^-$ $B220^-$	ND
	91 (313[b])	9.5	$CD3^+$ $CD4^+$ $CD8^+$ $B220^+$	ND
	97[b]	11.2	$CD3^+$ $CD4^-$ $CD8^+$ $B220^-$	0.11
	249	17.6	$CD3^-$ $CD4^-$ $CD8^-$ $B220^+$	ND
5×10^3	133	9.0	$CD3^+$ $CD4^+$ $CD8^+$ $B220^+$	0.18
	137[b]	6.8	$CD3^-$ $CD4^+$ $CD8^+$ $B220^-$	0.68
	183	7.5	$CD3^+$ $CD4^+$ $CD8^+$ $B220^-$	0.56
	189[b]	7.7	$CD3^-$ $CD4^+$ $CD8^+$ $B220^-$	0.19
	191[b]	8.0	$CD3^+$ $CD4^+$ $CD8^+$ $B220^+$	0.48
	192	10.0	$CD3^+$ $CD4^+$ $CD8^+$ $B220^-$	0.76
	209[b]	9.1	$CD3^+$ $CD4^+$ $CD8^+$ $B220^-$	0.80
	215	10.3	$CD3^-$ $CD4^+$ $CD8^-$ $B220^-$	0.29
	250	10.9	$CD3^-$ $CD4^-$ $CD8^-$ $B220^+$	ND
	258	10.0	$CD3^+$ $CD4^+$ $CD8^+$ $B220^-$	0.56

ND, not macroscopically detectable.
[a]Wild-type C57BL/6 thymus is 0.05 g ± 0.002 g (n = 20).
[b]Whole-genome massively parallel sequencing performed; m313 is the secondary recipient of m91 leukemic blasts.

occurs at the double-positive (DP) stage in the thymus. In contrast, there was a modest, but statistically significant, reduction in the number of sjTRECs present in splenocytes from mice transplanted with the low dose of progenitors when compared with both the high and mid cell doses. This is indicative of increased T cell expansion in the cohort of mice receiving the low dose of γc-expressing progenitors and is consistent with the observation of similar peripheral T cell reconstitution when compared with the mid dose group (Figure 2A).

Limiting Thymic Precursor Supply Affects the Size and Composition of the Thymus

We next sought to investigate the size and composition of the thymocyte population following transplantation. Thymocytes are classified into distinct stages based on expression of cell-surface markers, the earliest of which are DN for both CD4 and CD8. This DN population contains four sub-stages (DN1–DN4) identified by the level of cell-surface CD25 and CD44. Thymocytes then enter the DP stage where they are positive for both CD4 and CD8 before becoming single positive (SP; positive for either CD4 or CD8). At 6 weeks post-transplantation, for animals receiving either the high or low dose of wild-type progenitor cells, the total number of thymocytes was significantly reduced when compared to age-matched wild-type control animals not receiving bone marrow transplantation (Figure 3A). This demonstrates that transplantation even of high doses of wild-type progenitors leads to sub-physiological levels of thymocyte reconstitution. The difference between the high and low wild-type treatment groups was also significant; notably, however, the difference in the total number of thymocytes between these groups was only 7-fold, despite the 100-fold difference in the number of transplanted γc-expressing cells capable of progressing past the DN2 stage, confirmed by flow cytometry using Ly5.1 and Ly5.2 labeling to identify the γc-negative and γc-positive populations, respectively (Figure S1), indicating increased expansion in the low-dose cohort.

The contribution of DN, DP, and SP cells in the thymus was examined by flow cytometry, which revealed a significant reduction of DP cells in transplanted animals, proportional to the number of available wild-type progenitors from the bone marrow (Figures 3B and S2A). Interestingly, this was concomitant with a significant increase in the proportion of mature $CD4^+$ and $CD8^+$ SP cells, that also expressed CD3, in transplanted animals compared with wild-type controls, potentially indicating an increased need for early T cells to transition through the thymus ($p < 0.01$ for comparisons between all groups). Examination of the DN compartment showed that the proportion of cells in the DN1 stage was significantly increased in animals receiving the low dose of γc-progenitors compared both with mice receiving the high progenitor cell dose and with wild-type control animals (Figures 3C and S2B). A significant reduction was also observed for cells at the DN3 stage in mice receiving the low dose of γc-expressing progenitors.

The most evident difference between animals receiving the low dose of γc-expressing progenitors and those receiving the high progenitor dose or wild-type animals not receiving bone marrow transplantation was in the fold changes of thymocyte cell numbers within the DN niches. For the low-dose cohort, the ratio of DN2 to DN1 cells was significantly reduced (Figure 3D), possibly reflecting a rapid transition of cells from the DN2 niche, in an attempt to prevent lymphopenia in these animals. In striking contrast, there was a marked 6-fold increase in the ratio of DN4 to DN3 cells in mice receiving the low dose of γc-expressing progenitors, which may be indicative of a homeostatic mechanism to maintain the peripheral compartment size. It is possible that cells within the DN4 niche (i.e., negative for CD4, CD8, CD25, and CD44) could include progenitor cells of non-T cell lineages that reside in the thymus which may affect interpretation of DN ratios. It should also be emphasized, despite the differences observed in the relative proportion of each DN niche, particularly for animals receiving the low progenitor cell dose compared to wild-type control animals, that this is in concert with a marked reduction in the absolute number of cells in the thymus, and, therefore, all DN niches are diminished.

Molecular Characterization of Leukemic Clones

Genomic DNA was isolated from malignant blasts of affected animals and qPCR performed using primers to detect wild-type γc sequence, with wild-type sequence accounting for between 69.7% and 97.2% of the genomic DNA sample and correlating with the majority of each sample containing malignant cells. Importantly, this confirmed that all malignancies were derived from the transplanted $γc^+$ wild-type donor and not the γc-deficient donor or recipient cell populations, which is supported by the expression of T and/or B cell markers in the samples (Table 1).

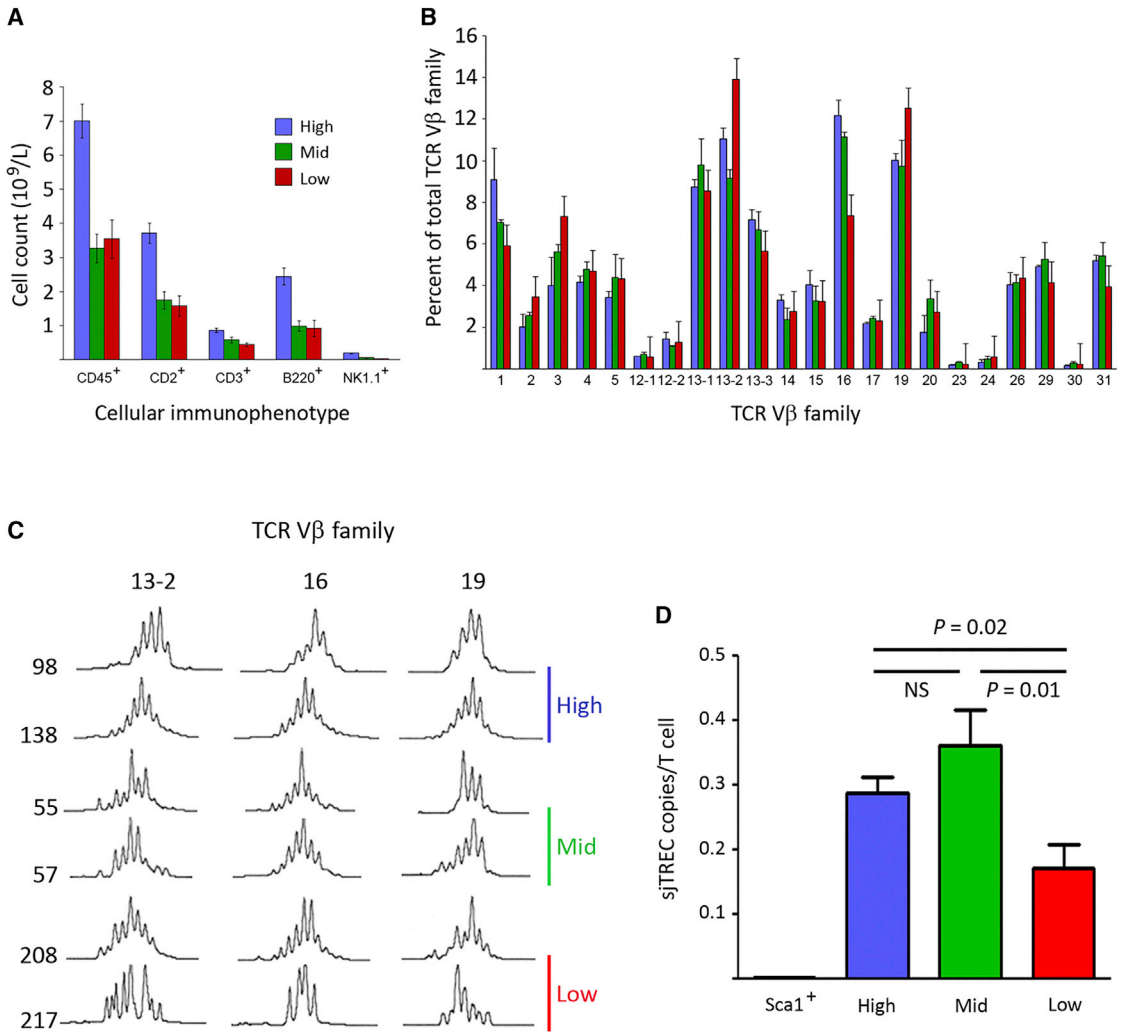

Figure 2. Immunological Reconstitution and T Cell Diversity under Conditions of Limiting Bone Marrow Progenitor Supply

(A) Total white cell counts were determined using peripheral blood samples taken from the tail vein at 16 weeks post-transplantation. Subset analysis was performed by staining with antibodies against murine CD2, CD3, CD45, B220, and NK1.1 and flow cytometric analysis. Data show mean ± SEM; n = 32, 31, and 30 for the high, mid, and low wild-type doses, respectively. (B) Peripheral blood was taken from mice at 15 weeks post-transplantation, and TCR V_β repertoire analysis was performed by qRT-PCR. The percentage of each TCR V_β family is indicated with results representing the mean of triplicate values for each group (n = 3). (C) CDR3 spectratypes of TCR V_β 13-2, 16, and 19 families in reconstituted mice transplanted with each of the three wild-type cell doses as indicated. (D) Quantitation of sjTREC in purified T cell populations from the spleen, 15 weeks following transplantation. Blue bars, high γc-expressing cell dose (5×10^5 cells); green bars, mid γc-expressing cell dose (5×10^4); red bars, low γc-expressing cell dose (5×10^3 cells).

Whole-genome sequencing (WGS) was performed on selected leukemic clones that contained a high proportion (≥75%) of malignant cells (Figure 4; m97, m137, m189, m191, m209, and m313) to identify potential common mutational signatures. Microarray analysis was also performed on five of the six samples (the quality of RNA for sample m137 was not sufficient for analysis). Of the 407 mouse orthologs contained in the Sanger cancer consensus genes database (http://cancer.sanger.ac.uk/census/), 14 (3.4%) displayed expression levels that were altered >2-fold when compared to wild-type thymocytes (*Brca2*, *Card11*, *Ccnd1*, *Gnaq*, *Hmga1*, *Il21r*, *Itk*, *Jazf1*, *Notch1*, *Nr4a3*, *Pdgfrb*, *Recql4*, *Rel*, and *Tfrc*). All sequenced samples except m313 (adoptive transfer recipient) showed evidence of substantial copy number decreases on the X chromosome, in comparison to Sca1$^+$ bone marrow progenitors. Also, substantial copy number gains on chromosome 15 were shown to be common for mice receiving the low dose of γc-positive progenitors (m137, m189, m191, and m209). This evidence is in keeping with the data of Martins et al., who had observed gains on chromosome 15.[10] Interestingly, one sample (m209) also displayed large copy number gains on chromosome 14 (Figure 4).

Activating *Notch1* mutations were identified by WGS in each of the samples, comprising either a 5′ deletion or mutations within the sequence encoding the proline, glutamate, serine, and threonine

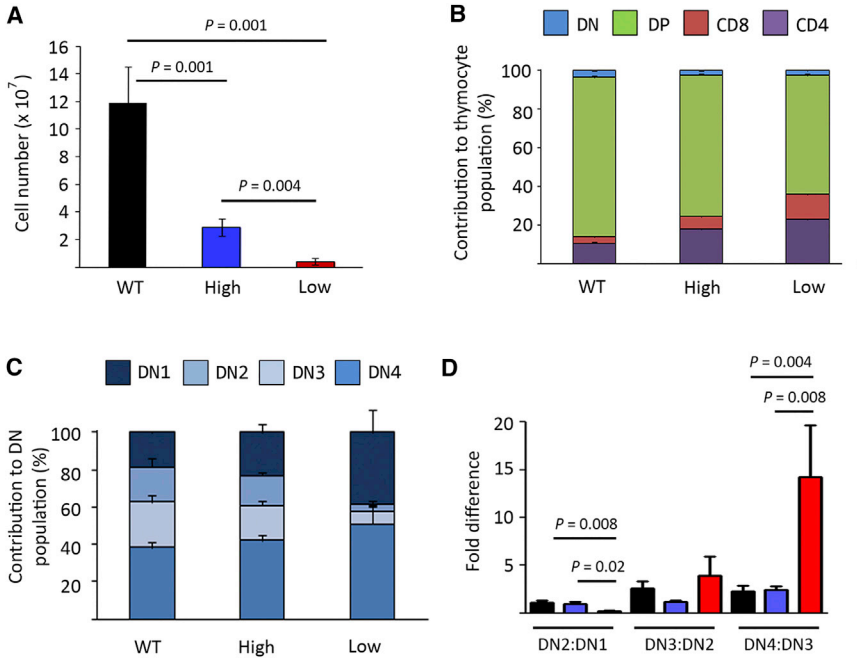

Figure 3. Thymic Size and Composition under Conditions of Limiting Bone Marrow Progenitor Supply

(A) Size of the thymocyte population at 6 weeks post-transplantation in C57BL/6 control animals (black bar) or mice receiving either the high (blue bar) or low-dose (red bar) of γc-expressing progenitor cells. (B) Percentages of early T cells within the thymus at 6 weeks post-transplantation in age-matched controls and animals receiving the high or low dose of γc-expressing progenitors; DN, blue; DP, green; SP $CD8^+$, red; SP $CD4^+$, purple. (C) Percentages of cells within the DN niche at 6 weeks post-transplantation in age-matched controls and animals receiving the high or low dose of wild-type progenitors; DN1, darkest blue; DN2, mid blue; DN3, light blue; DN4, dark blue. (D) Ratios of cells in the DN niches (DN2:DN1, DN3:DN2, and DN4:DN3) at 6 weeks post-transplantation in age-matched controls (black bars) and animals receiving the high (blue bars) or low (red bars) dose of wild-type progenitors. Values represent the mean ± SEM with n = 7, 6, and 6 for age-matched controls and high and low γc-expressing progenitor cell doses, respectively.

(PEST) domain located in exon 34 (Figure 5A). Sanger sequencing across the affected regions confirmed these mutations and gene expression profiling by microarrays identified *Notch1* upregulation in malignant samples (3.5-fold, false discovery rate [FDR] adjusted p value = 0.012). Of the six samples investigated, five contained the 5′ deletion and five contained a mutation in exon 34, with four of the six samples carrying both lesions. We also observed exon 34 deletions in our previous study.[5] Similar mutations have been identified in leukemia samples generated under conditions of thymic progenitor cell deprivation.[10] To investigate the presence of activating mutations in the *Notch1* proto-oncogene in our other samples, DNA sequence analysis was performed across the breakpoint of the 5′ deletion as well as the PEST, transactivation (TAD), or heterodimerization (HD) domains. Further, activating *Notch1* mutations (5′ deletions and/or PEST domain mutations) were identified in the remaining tumors (those not subjected to WGS) from mice transplanted with the low dose of γc-expressing progenitors (Table 2; Figures 5B and 5C).

The impact of activating mutations in *Notch1* was investigated by using qRT-PCR directed at the downstream targets, *c-myc*, *Dtx1*, and *Hes1*. In the malignant blasts examined (n = 5), elevated levels of these transcripts were observed when compared to normal wild-type thymocytes; *c-myc*, *Dtx1*, and *Hes1* were found to be upregulated by 6.85 ± 1.80, 2.47 ± 0.54, and 2.78 ± 0.26-fold, respectively (data not shown). Upregulation of *Hes1* (9.78-fold, FDR = 0.021) and *c-myc* (3.25-fold, FDR = 0.073) in malignant blasts was also detected by microarray analysis.

DISCUSSION

We have identified limiting bone marrow progenitor supply to the thymus as an initiator of lymphoid malignancy in mice. Importantly, this oncogenic risk is cell dose dependent, occurs within cell dose ranges that support immunological reconstitution, and does not require the complete absence of progenitor cell migration from the bone marrow as previously observed in thymic grafting studies,[8,10] making this feature of our model unique. Based on existing evidence, the mechanism underlying oncogenesis is theorized to have two critical components. The first is the induction of a transformation-prone self-renewal phenotype in a subset of thymocytes as a homeostatic response to an inadequate supply of progenitors from the bone marrow.[7–9] The second is reduced competitive pressure on this at-risk population for thymic niche space from differentiation-committed thymocytes progressing through lymphoid ontogeny.[10] The proposed combined effect would be an increase in the number and residency time of transformation-prone thymocytes, leading to a correspondingly higher probability of cells within this population being subject to oncogenic second hit events, such as activating mutations in *Notch1*.

In an effort to phenocopy gene therapy for SCID-X1 in our model system, mice were reconstituted with serially fewer wild-type bone marrow progenitor cells, used as surrogates for gene-corrected cells, against a background of γc-deficient progenitors adjusted to maintain a constant total cell dose in all treatment groups. In this context, the inverse correlation observed between the incidence of T-lymphoid malignancy and wild-type progenitor cell dose is consistent with a failure of γc-deficient cells to progress to the point in T cell ontogeny, the DN3 niche, where competitive pressure on tumor-prone self-renewing thymocytes has been hypothesized to exert a tumor-suppressive effect.[10]

When we initially observed T-lymphoid oncogenesis, independent of insertional mutagenesis in our earlier gene therapy study in SCID-X1

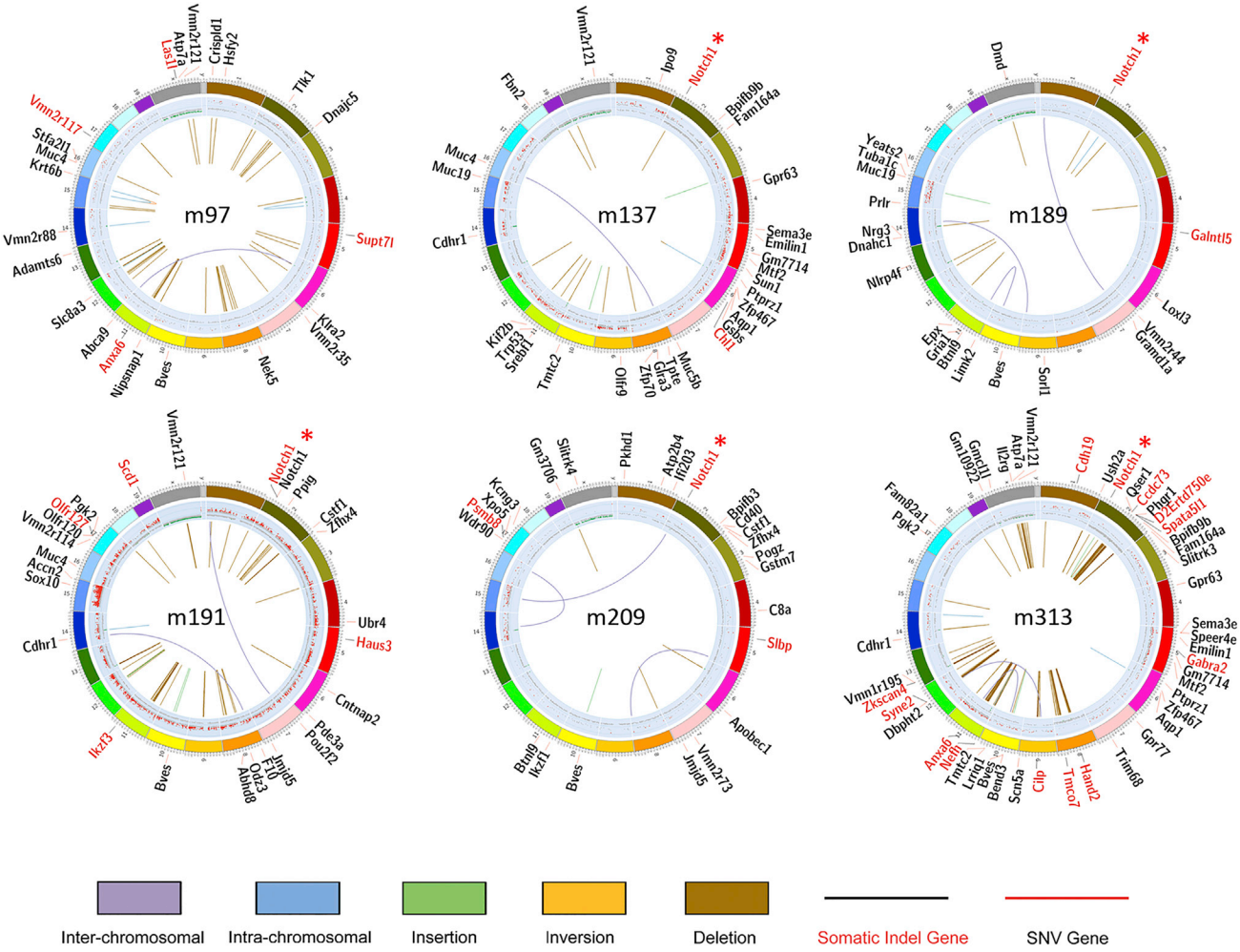

Figure 4. Whole-Genome Sequence Analysis of Selected Lymphoid Malignancies

Circos plots representing six malignant genomes are shown with notable mutations (somatic SNVs and InDels) compared to wild-type Sca1$^+$ progenitors indicated. The three circles in each plot, from outermost inward, represent the mouse chromosomes, copy number alterations (red dots >1.5-fold, green dots <0.5-fold), and structural rearrangements (rearrangement types are depicted with different colors, indicated under the bottom panel). Genes with SNV (red) and small InDels (black) are labeled on the circos plots, except for mutations in Chr8 and Chr11 of m313 owing to space limitations. An asterisk indicates InDels identified in the PEST domain of *Notch1*.

mice,[5] we favored replicative stress as a possible tumorigenic mechanism. For this reason, an effort was made to examine the differing effects of limiting progenitor cell doses on the extent and location of the homeostatic cellular expansion during T cell ontogeny by assessing TCR diversity and number sjTREC in peripheral blood T cells, although an analysis of whether there were differences in the percentages of naive and memory peripheral T cells, with an increase in the latter indicative of homeostatic proliferation under conditions of lymphopenia,[13] was not performed. Despite 100-fold fewer cells capable of progression past the DN2 stage of thymic ontogeny, and competent for lymphoid ontogeny in the low-dose wild-type progenitor cell treatment group, reduction in the resultant peripheral T cell compartment size was only in the order of 2-fold. This is clearly indicative of higher levels of cellular replication during T cell ontogeny in these animals. While this represents a 50-fold change in the relative size of the input progenitor and output peripheral T cell populations, the relative difference in the absolute number of cell divisions required to achieve this, in an exponentially expanding population, is much smaller.

Accepting that the dynamics of thymic homeostasis are complex,[14,15] this argues against the oncogenic risk observed at limiting progenitor cell doses being a simple function of the cumulative burden of somatic mutations acquired during individual cell division events. Data from TCR diversity and sjTREC analysis in peripheral blood and splenic T cells, respectively, also provide similar arguments supporting this point. Relatively well-preserved TCR diversity, in concert with TREC-based evidence for a 2-fold replicative expansion of T cells following TCRα rearrangement in mice receiving 100-fold fewer γc-expressing progenitors, provides evidence of homeostatic expansion both before and after the DP stage of T cell ontogeny. While

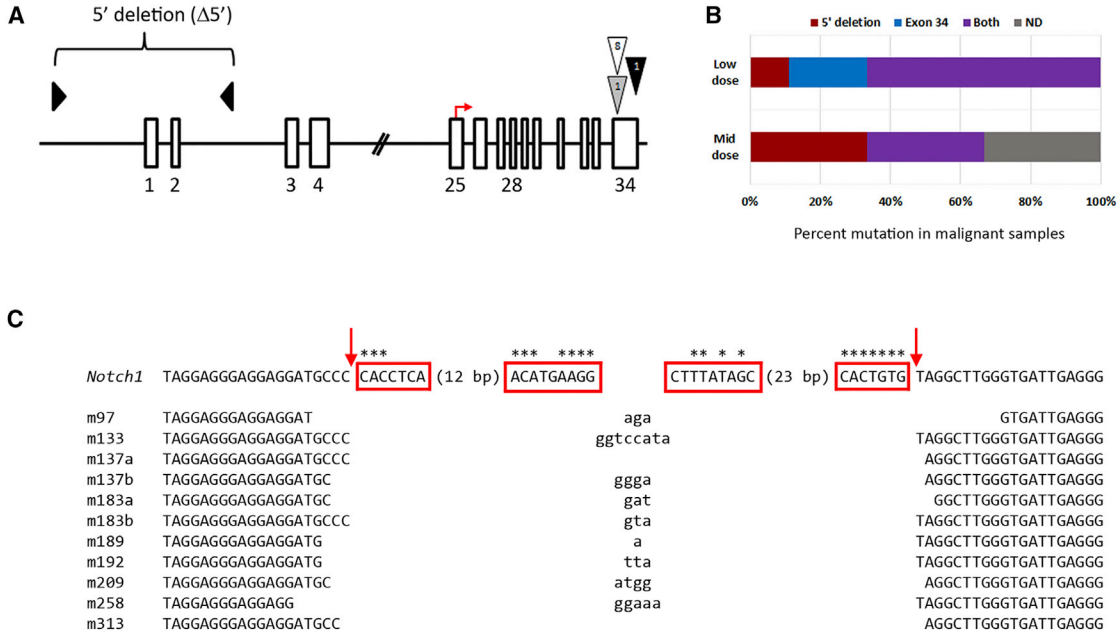

Figure 5. Molecular Analysis of Lymphoid Malignancies Observed under Conditions of Limiting Bone Marrow Progenitor Supply

(A) Schematic representation of murine *Notch1* indicating the position of the 5′ deletion (Δ5′) and activating mutations in exon 34 affecting the PEST domain (triangles). The numbers of malignancies with exon 34 mutations are indicated; white, frameshift deletions; gray, frameshift addition; black, single nucleotide substitution resulting in a premature stop codon. The location of a cryptic promoter (exon 25) is designated by the arrow. (B) Graph showing the frequency and type of *Notch1* mutations (Δ5′ and/or PEST domain) identified in T cell malignancies at the low (n = 9) and mid (n = 3) wild-type progenitor cell doses. ND, not detected. (C) The *Notch1* germline sequence flanking exons 1 and 2 is indicated in the top row and samples, with evidence of N nucleotide addition (in lower case), shown below. Sequences in red rectangles are heptamer-(CACAGTG) or nonamer-like (ACAAAAACC) motifs separated by 12- or 23-bp spacers and asterisks indicate canonical nucleotide residues.[53] Arrows designate the sites of *Rag*-mediated DNA breakage.

this supports a 50-fold relative expansion prior to, and a 2-fold expansion after the DP stage, in an exponentially growing population, the difference in the absolute number of cell divisions occurring before and after the DP stage is likely to be relatively small. Further analyses, including whether there is increased proliferation of wild-type progenitors, compared to the immunodeficient populations, or a greater number of early thymic progenitors (ETPs) would contribute to the understanding of the extent and location of the homeostatic cellular expansion during T cell ontogeny in our model. Early thymic progenitors, identified by high levels of cKit on their surface (cKit^{high} cells), have been shown to support long-term thymopoiesis in intrathymic transplantation studies.[13,16] If cell division itself was a strong risk factor for transformation, then one would expect a high proportion of such events to occur in more mature T cells, which is unsupported by existing evidence.[7–11]

When considering the possible relevance of these murine data to the oncogenic mechanisms operative in early human SCID-X1 gene therapy trials, it is important to emphasize that murine cells are inherently more transformation-prone than human cells,[17] and to our knowledge there is no evidence to suggest that limiting thymic precursor supply in humans carries oncogenic risk through the induction of thymocyte self-renewal. Indeed, based on clinical experience in allogeneic stem cell transplantation for SCID phenotypes including SCID-X1, Qasim et al. have argued against oncogenic risk being associated with a lack of bone marrow progenitor supply to the human thymus.[18] They point to the absence of reports of T cell malignancy in patients with long-term thymopoiesis, despite single-lineage donor T cell recovery, which is considered indicative of thymic, but not bone marrow engraftment.

A further important point is that oncogenesis in early human clinical trials, using conventional γ-retroviral vectors to treat SCID-X1, chronic granulomatous disease (CGD),[19] and Wiskott-Aldrich syndrome (WAS)[20] invariably involved insertional mutagenesis, while oncogenic adverse events have not subsequently been observed with SIN γ-retroviral or SIN lentiviral vectors lacking strong viral enhancer-promoter elements. Nevertheless, we argue that insertional proto-oncogene activation in human hematopoietic progenitors, as reported in early SCID-X1 trials, is likely capable of inducing transformation-prone thymocytes. This is supported by the observation that deliberate *Lmo2* overexpression in mice can induce thymocyte self-renewal without a homeostatic drive being exerted by a limiting or absent progenitor supply.[11] Once such cells arise in the human thymus, albeit by an iatrogenic mechanism, it is plausible that γc-deficient human thymic progenitors, akin to their murine counterparts, also fail to exert a tumor suppressor effect through competitive pressure. Thus, the parallels of our findings, and those of

Table 2. Summary of *Notch1* Mutations Identified in Lymphoid Malignancies

Wild-Type Cell Dose	Mouse	5′ Deletion (Δ5′)	Exon 34 Mutation[a]
5×10^4	50	ND	ND
	91	ND	ND
	97	yes	ND
	249	ND	ND
5×10^3	133	yes	G > T 7172, insertion TTAC 7173
	137	yes[b]	insertion CA 7283, G > C 7284
	183	yes[b]	C > T 7345
	189	yes	G > C 7172, insertion ACCT 7173
	191	ND	G > A 7284, insertion AATCGAAGGGC 7285
	192	yes	ND
	209	yes	insertion AGTCTGAAGA 7362
	215	ND	insertion T 7146
	250	ND	ND
	258	yes	deletion CA 7476
NA[c]	313	yes	insertion CA 7283, G > C 7284

ND, not detected by sequencing amplicon clones; NA, not applicable.
[a]Frameshift mutations all result in the introduction of a premature stop codon and associated loss of the PEST domain; indicated position is relative to GenBank accession AB100603.1. Mutations were not identified in the HD or TAD domains.
[b]Two break points were identified.
[c]m313 is the secondary recipient of m91 leukemic blasts.

previously reported thymic transplant studies, to the human gene therapy experience occurs once the cells acquire a capacity for self-renewal, induced by either limiting precursor supply or by proto-oncogene activation. This also provides an alternative explanation for the suggested oncogenicity of γc itself that has been the topic of much debate.[21,22]

An intriguing question arising from the tumor suppressor hypothesis is whether there might be disease-specific differences among disorders affecting T cell ontogeny in the capacity of thymocytes to exert tumor-suppressive effects through cell competition. For example, in gene therapy trials for ADA-SCID, using conventional γ-retroviral vectors to transduce bone-marrow-derived $CD34^+$ cells, there have been no reports of T cell leukemia, despite the frequent observation of integration events in *LMO2* and other proto-oncogene loci.[23] Unlike γc-deficient thymocytes, which fail to progress beyond the DN2 thymic niche, ADA-deficient thymocytes are able to progress through thymic ontogeny when the thymic microenvironment is sufficiently metabolically detoxified,[24] thereby providing a possible tumor suppressor effect in more distal thymic niches by competing with transduced cells carrying insertional proto-oncogene activation events (Figure 6). While alternative hypotheses exist to explain the differing risk of oncogenesis in early gene therapy trials for SCID-X1 and ADA-SCID, none provide a unifying conceptual framework. For SCID-X1 these include evidence for cooperativity between *Lmo2* and γc expression in the thymus with double transgenic mice showing accelerated development of T cell malignancy, strikingly in association with *Notch1* mutations.[25] For ADA-SCID, these include the possibility that the progenitors transduced in bulk $CD34^+$ populations might be more differentiated than for SCID-X1, and that the level of vector-encoded ADA expression might be insufficient to support the development of a T cell leukemic phenotype, which has been shown to be associated with increased ADA expression.[26] Another notable difference between these two gene therapy trials was the use of sub-ablative busulfan conditioning in ADA-SCID patients, which is known to increase the level of bone marrow engraftment.[27] It is therefore conceivable that increased bone marrow engraftment may lead to increased thymic seeding with a resultant reduction in oncogenic risk. Increasing the level of myeloablative condition in our model might also reduce the incidence of malignancy for a given cell dose. A further challenge is to reconcile the concept of cell competition as a tumor suppressor mechanism in the thymus with the occurrence of T cell leukemias in a gene therapy trial for Wiskott-Aldrich syndrome (WAS) using a conventional γ-retroviral vector.[20] Six of ten treated patients developed T-ALL with dominant *LMO2* clones identified in each case. Several of the leukemias also had secondary mutations in the proto-oncogenes *TAL1* and *LYL1*, both of which are known to be associated with T-ALL. Similar to ADA-SCID, there is no absolute block to T cell ontogeny in the thymus in WAS, although abnormalities of T cell development have been implicated in this condition.[28–30] Of particular relevance, the WAS protein (WASP) has been shown to be important for double-negative to double-positive cell transition that may partly be explained by reduced cycling of DN3 cells. Further, it has been suggested that in the absence of WASP, the decreased migratory responses and increased percentage of single positive cells implies retention of these cells in the thymus.[29] It therefore remains plausible that this could result in reduced competitive pressure on thymocytes rendered pre-leukemic by insertional proto-oncogene activation. Data derived from our model are certainly consistent with this possibility given our demonstration that lymphoid oncogenesis does not require a complete block in bone marrow progenitor supply and, at least in mice, is observed at wild-type progenitor cell doses that are sufficiently high to reconstitute the peripheral T cell compartment. Ultimately the hypothesis that ADA and WAS protein-deficient thymocytes have differing capacities to act as tumor suppressors in the thymus, through cellular competition, requires experimental evaluation and could be addressed in the model system we describe in the current report using γc-deficient cells.

Ultimately, despite evidence that insertional proto-oncogene activation was necessary, but not sufficient, for development of T cell leukemias in early gene therapy trials for SCID-X1, the second hit events required for transformation, which we hypothesize are suppressed by cellular competition, show considerable similarity in mice and humans, most notably activating mutations in the PEST domain of NOTCH1.[3,4] These, predominantly frameshift, mutations result in the production of a truncated protein and persistent activation of Notch1 downstream targets[5,31,32] and are consistent with those identified in our previous gene therapy model.[5] Interestingly, in contrast

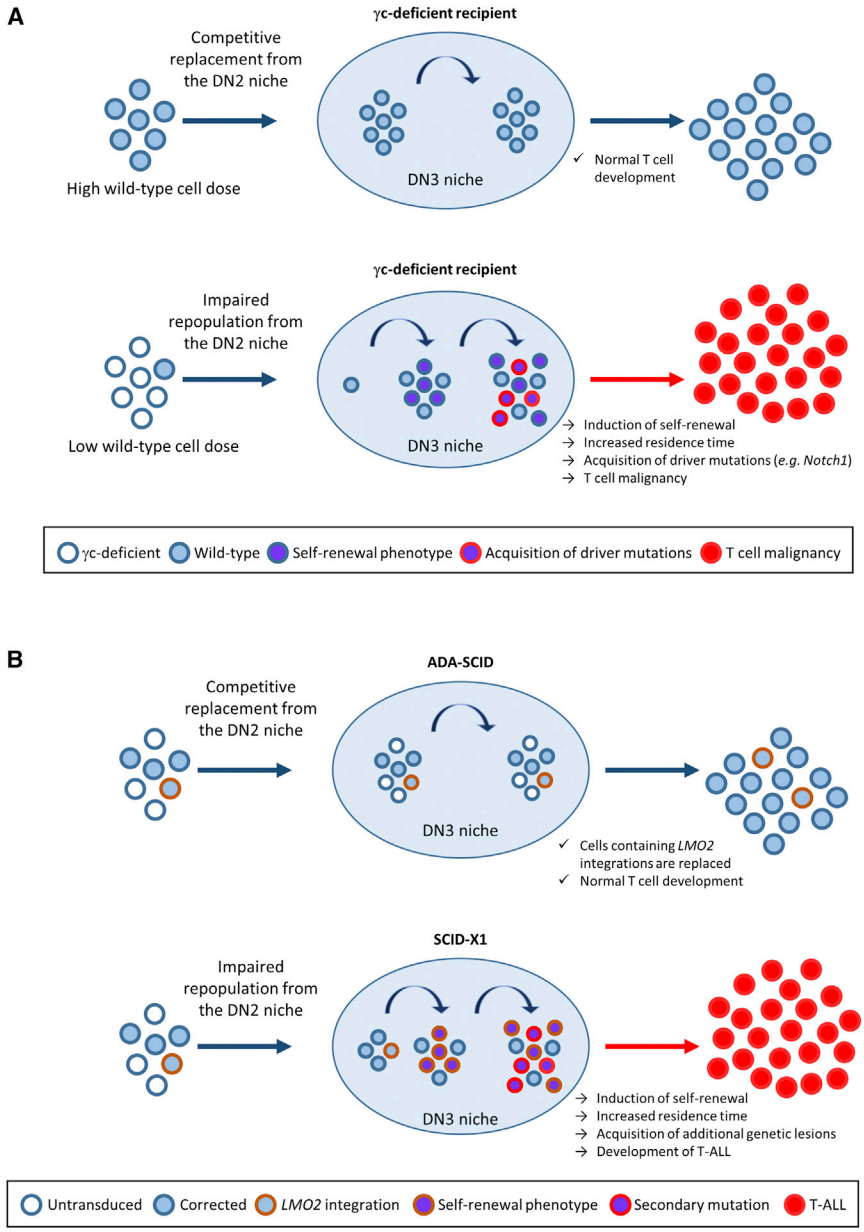

Figure 6. Hypothetical Models of Competitive and Impaired Replacement in γc-Deficient Mice and Human Clinical Trials of ADA-SCID and SCID-X1, where the Acquisition of an At-Risk Phenotype May Lead to Malignant Transformation

(A) The thymus is continuously supplied from the bone marrow when transplanted with a high dose of wild-type cells, thereby replacing thymus-resident progenitor cells. When a low dose of wild-type cells are transplanted; however, there is reduced competition possibly leading to self-renewal of thymus-resident progenitors, increased residence time in the thymus, and the potential to acquire additional genomic mutations such as those observed in *Notch1*. (B). In ADA-SCID, cells containing deleterious integrations migrate out of the thymus by normal cellular replacement, because cells that are not gene-modified are capable of progressing past the DN2 niche. For SCID-X1, however, cells containing similar integrations in *LMO2* may have self-renewal potential. These cells could then be retained in the thymus for extended time periods because of reduced progenitor cell migration (because cells that have not been gene-corrected are unable to progress past the DN2 niche due to a lack of interleukin-7 [IL-7] signaling) and may acquire additional genetic lesions in some patients.

to the findings of Martins et al.,[10] mutations in the HD or TAD domains were not present in our samples. This is likely due to the *Notch1* 5′ deletion being functionally similar to a HD mutation (see below); thus, the presence of a 5′ deletion and HD mutation in the same cell would be mechanistically redundant.[33] Finally, consistent with the strong association of *Notch1* mutations and cases of T cell leukemia and lymphoma[34] in the two malignancies not expressing T cell-surface markers (m249 and m250), *Notch1* mutations could not be detected by sequencing amplicon clones. This was in contrast to observations by Martins et al., where all leukemias had an immature CD8 single-positive (ISP)/double-positive (DP)-like surface phenotype[10] and possibly reflect inherent differences between these two models, notably the source of thymic progenitors being either whole thymus or, in our model, more immature bone marrow progenitor cells.

In samples with the 5′ deletion, an aberrant *Notch1* mRNA initiated from a cryptic promoter in exon 25 produces an active intracellular Notch1 protein that is independent of ligand binding and γ-secretase cleavage[35–37] and therefore constitutively expressed (Figure 5A). These mutations have been shown to result from illegitimate V(D)J recombination[36] and, in our study, may have arisen from a failure of cells to exit the thymus as a result of reduced progenitor cell supply. Notably, although 5′ deletions in *NOTCH1* were not identified in SCID-X1 patient samples, they did contain deletions in the tumor suppressor gene locus cyclin-dependent kinase inhibitor 2A (*CDKN2A*), also shown to be the consequence of aberrant V(D)J recombination;[33] however, similar *Cdkn2a* deletions were not found in the six tumor genomes analyzed by WGS in this study. Further evidence of illegitimate V(D)J recombination was identified in our model by whole-genome sequencing, where both α/β and γ/δ recombination events were present in all six tumor genomes analyzed (data not shown). This is in keeping with the observation that the T-ALL that developed in some patients in the SCID-X1 trials arose from both the α/β and γ/δ T cell populations.

In summary, our studies support the role of regenerating thymic precursors in the thymus leading to further genetic abnormalities that

predispose to cancer. These findings help explain the differences in cancer risk in diseases treated with gene therapy based on the relative size of the thymic precursor pool and the need for regenerative thymic clones that are predisposed to malignant transformation. Although there is currently no evidence that limiting thymic precursor supply is a risk factor for lymphoid malignancy in humans, our data provide a compelling conceptual framework that could explain why T cell leukemia was observed in early SCID-X1 trials but not in ADA-SCID patients, despite both groups containing integrations near proto-oncogenes such as *LMO2*.

MATERIALS AND METHODS

Animals

IL2RG$^{-/-}$ mice[12] were obtained from The Jackson Laboratory, $\gamma c^{-/-}$ Rag2$^{-/-}$ mice were kindly provided by Professor Stephen Nutt (Walter and Eliza Hall Institute, Parkville, Australia), and C57BL/6 mice were obtained from the Animal Resources Centre (ARC). All experimental procedures were approved by the Animal Ethics Committee of the Children's Medical Research Institute and The Children's Hospital at Westmead.

Progenitor Cell Isolation and Transplantation

Recipient $\gamma c^{-/-}$Rag2$^{-/-}$ mice were exposed to sublethal (6 Gy) irradiation using a Gammacell 40 Exactor (MDS Nordion). Bone marrow was harvested from 8- to 10-week-old IL2RG$^{-/-}$, C57BL/6, or C57BL/6 Ly5.1 congenic mice, and Sca1^{+} progenitor cells were isolated using the EasySep SCA1 positive selection kit (STEMCELL Technologies), resuspended in 200 μL RPMI 1640 medium (Life Technologies) and injected intravenously into recipient mice via the tail vein.

Analysis of TCR Repertoire and CDR3 Spectratyping

At 15 weeks post-transplantation, individual TCR V_β families in peripheral blood were detected using qRT-PCR and primers specific for the TCR β chain.[38] All analyses were performed in triplicate as previously described.[39] The TCRVβ repertoire diversity of the six most highly represented TCR V_β families was subsequently analyzed by CDR3 spectratyping as outlined previously.[38]

Quantitation of Signal Joint T Cell Receptor Excision Circles

At 16 weeks post-transplantation, T cells from reconstituted mice were separated using the EasySep Mouse CD90.2/Thy 1.2 Positive Selection Kit (STEMCELL Technologies) and genomic DNA isolated using the Gentra Puregene cell kit (QIAGEN). Signal joint T cell excision circles (sjTREC) were detected by using real-time qPCR with the following primer and probe set; forward 5′-CATTGCCT TTGAACCAAGCTG-3′; reverse, 5′-TTATGCATAGGGTGCAG GTG-3′; probe 5′-FAM-CGGCAGGGTTTTTGTAAAGGTGCTC ACTT-QSY-3′.[40] Reactions were performed on a Rotor-Gene 6000 (QIAGEN), and the number of sjTREC within each sample was determined by using the comparative C_t method and a sample containing a known number of sjTREC copies, diluted in murine 3T3 cell genomic DNA. The constant gene segment of the *TCRA* gene (Cα) was used to compensate for variations in input DNA with the following primer and probe set: forward 5′-TGACTCCCAAATCAATGTG-3′; reverse, 5′-GCAGGTGAAGCTTGTCTG-3′; probe 5′-FAM-TGCTGGACAT GAAAGCTATGGA-QSY-3′.[41]

Flow Cytometric Analysis

Cells from the bone marrow, thymus, spleen, liver, and peripheral blood were stained and analyzed on a FACSCanto (BD Biosciences) running FACSDiva (v.6.1.3) and FlowJo (v.7.6.1, FlowJo LLC) software. Lymphocytes were identified and gated based on their forward-scattered light (FSC) and side-scattered light (SSC) profiles. Cell suspensions were treated with ACK lysis buffer (150 mmol/L NH_4Cl, 10 mmol/L $KHCO_3$, and 0.1 mmol/L disodium EDTA) and then stained with the following conjugated antibodies: B220-APC-Cy7 (BD Biosciences), CD2-FITC (BD Biosciences), CD3ε-PE (BD Biosciences), CD3ε-Alexaflore 647 (BD Biosciences), CD4-FITC (Caltag Laboratories), CD8a-APC (Caltag Laboratories), CD8a-Alexaflore 647 (BD Biosciences), CD25-FITC (BD Biosciences), CD44-PE (BD Biosciences), CD45-APC (BD Biosciences), Ki-67-FITC (BD Biosciences), Ly5.1-PerCP-Cy5.5 (BD Biosciences), Ly5.2-PerCP-Cy5.5 (BD Biosciences), NK1.1-APC (Caltag Laboratories), and Sca1-Alexaflore 647 (BD Biosciences).

Histology

Tissue was dissected from C57BL/6 control or transplanted $\gamma c^{-/-}$ Rag2$^{-/-}$ recipient mice and fixed in 10% buffered formalin (Sigma-Aldrich). Paraffin-embedded sections (5 μm) were stained with H&E and evaluated by light microscopy. Images were captured from a Zeiss Axio Imager.A1 Microscope (Carl Zeiss MicroImaging) using a Spot enhanced camera (Diagnostic Instruments, SciTech) running Spot Software (v.4.0.1).

qPCR to Determine Leukemic Origin

To determine whether malignancies were donor or recipient in origin, genomic DNA was isolated using the Gentra Puregene cell kit and qPCR performed using primers to either the human γc (5′-CTTTATTGATAACGATCTATATCCCTCACCC-3′ and 5′-CTCCACTCTGCAGAGTCTATGGAATCC-3′) or bacterial neomycin phospho-transferase (5′-CTTGGGTGGAGAGGCTA TTC-3′ and 5′-AGGTGAGATGACAGGAGATC-3′) gene. Reactions were performed on a RotorGene 6000 (QIAGEN) using the QuantiTect SYBR Green PCR kit (QIAGEN) and standardized using primers to the murine *titin* gene (5′-AAAACGAGCAGTGACG TGAGC-3′ and 5′-TTCAGTCATGCTGCTAGCGC-3′) by the comparative Ct method.

Primary Sequence Analysis and Variation Detection

Genomic DNA from six lymphoid tumors and one control sample of C57BL/6 Sca1^{+} progenitor cells were sequenced at the Beijing Genomics Institute (BGI), using HiSeq2000. Whole-genome sequencing was achieved to 30 times coverage and a comparative analysis between the control sample and the tumors, to call tumor-specific somatic single nucleotide variants (SNVs), somatic copy number variations (CNVs), short insertions/deletions (InDels), and structure variant (SV) mutations, was performed. BGI's cancer genomics

bioinformatics pipeline was applied for sequencing analysis and variation detection (http://www.bgitechsolutions.com/). Paired-end reads were aligned by Burrows-Wheeler aligner (BWA)[42] to the mouse mm9 reference genome. All BAM files were processed to identify duplicates using the Picard MarkDuplicates tool from the Broad Institute. SNVs were detected using VarScan,[43] InDels were called by SAMtools,[44] CNVs were called by BGI's proprietary method CNV_Detection, and SVs were called by CREST.[45] Copy number ratios <0.5 were considered as deletions and >1.5 as amplifications. ANNOVAR software[46] was used to annotate the variant results. The Integrative Genomics Viewer (IGV) 2.3[47] was used to visually inspect sequence reads. BAM files and associated metadata in XML format have been uploaded to the European Nucleotide Archive (ENA; http://www.ebi.ac.uk/ena) under the study identification number PRJEB8006.

Gene Expression Arrays

Total RNA for expression analysis was isolated using the RNeasy Mini Kit (QIAGEN), and transcriptome profiling was performed by The Ramaciotti Centre for Gene Function Analysis (University of New South Wales). Briefly, total RNA samples (500 ng/sample) were amplified and labeled according to the manufacturer's instructions (Affymetrix). Amplified RNA was quantified using a NanoDrop (Thermo Scientific) and distribution of the amplified material was analyzed in a 2100 Bioanalyzer (Agilent). Amplified cRNA was hybridized onto Affymetrix mouse 2.1 gene arrays; the arrays were scanned and expression measurements extracted using the Affymetrix Expression Console v.1.3 software. Microarray data have been deposited at ArrayExpress (http://www.ebi.ac.uk/arrayexpress/) under the accession number E-MTAB-3159.

Gene Expression Data Analysis

Robust Multi-array Average (RMA) was applied to normalize the expression data,[48] and the remaining analysis was carried out using *Bioconductor* package[49] in the R statistical language 3.01. Empirical Bayes statistics for differential expression were calculated using *limma* 3.16.6.[50] p values were adjusted by Benjamini & Hochberg's method to account for multiple test correction.[51] Genes with expression change $\geq$2-fold and adjusted p value (FDR) $\leq$0.05 were considered as differentially expressed.

Identification of *Notch1* Gene Mutations and Structural Variations

Mutations within the PEST, TAD, or HD domains of *Notch1* were identified by sequencing PCR products amplified using *Pfu* DNA polymerase (Promega). Primers spanning exons 26, 27, and 34, where the HD, TAD, and PEST domains are located, are described elsewhere.[31] The presence of structural variations in *Notch1* identified by WAS was confirmed by PCR amplification using Phusion high-fidelity DNA polymerase (New England Biolabs) and primers adjacent to the 5′ and 3′ break points (5′- CAGTCAGGAGTGGTGGATCC-3′ and 5′-GGCTTGGTCTAGTGCTCCTG-3′). In cases where the PCR product contained more than one amplicon, the PCR product was cloned into pGEM-T Easy (Promega), and the sequence of individual clones was determined.

qRT-PCR for *Notch1* Downstream Targets

Total RNA was extracted using the RNeasy mini kit (QIAGEN) from lymphoblastic cells or from wild-type thymocytes and cDNA synthesized from 1 μg total RNA by using the Superscript III first-strand synthesis Supermix kit (Life Technologies). To determine whether mutations in *Notch1* affected expression of downstream target genes, qRT-PCR was performed on a RotorGene 6000 using *c-myc* (5′-CTGTTTGAAGGCTGGATTTCCT-3′ and 5′-CAGCACCGA CAGACGCC-3′), *Dtx1* (5′-TGCCTGGTGGCCATGTACT-3′ and 5′-GACACTGCAGGCTGCCATC-3′), and *Hes1* (5′-AAGACGG CCTCTGAGCACA-3′ and 5′-CCTTCGCCTCTTCTCCATGAT-3′) primers[52] using the Brilliant III Ultrafast SYBR green QPCR master mix (Agilent Technologies). Expression levels were standardized using primers to the β-actin gene (5′- CTAGACTTCGAGCAGG AGATGGC-3′ and 5′- TCTGCATCCTGTCAGCAATGCC-3′) by the comparative Ct method.

Statistical Analysis

Results were analyzed by the Wilcoxon rank-sum (Mann-Whitney) (http://www.socscistatistics.com/tests/mannwhitney/default2.aspx) or Fisher's exact test (http://www.graphpad.com/quickcalcs/contingency1.cfm). For comparison of population survival, cohorts of mice were evaluated using Kaplan-Meier analysis (GraphPad Prism v.5.04). Values represent the mean ± SEM and results considered significant when $p < 0.05$.

SUPPLEMENTAL INFORMATION

Supplemental Information includes two figures and can be found with this article online at http://dx.doi.org/10.1016/j.omtn.2016.11.011.

AUTHOR CONTRIBUTIONS

Conceptualization, S.L.G., C.V.H., and I.E.A.; Methodology, M.H.; Formal analysis, S.L.G., S.H.Y.L., E.T.T., and J.W.; Investigation, S.L.G., C.V.H., and S.H.Y.L.; Writing – Original Draft, S.L.G. and I.E.A.; Writing – Review and Editing, S.L.G., C.V.H., E.T.T., J.W.A., S.S.T., R.R.R., M.P.M., M.C., A.J.T., S.I.A., and I.E.A.; Visualization, H.C.L.; Funding Acquisition, S.L.G., C.V.H., R.R.R., M.P.M., A.J.T., S.I.A., and I.E.A.

CONFLICTS OF INTEREST

There are no conflicts of interest to disclose.

ACKNOWLEDGMENTS

We thank Professor Stephen Nutt (Walter and Eliza Hall Institute, Parkville, Australia) for providing the $\gamma c^{-/-}Rag2^{-/-}$ mice and the BioResources staff of Children's Medical Research Institute for assistance in maintaining the animal lines used in this study. This work was supported by a project grant (632657) from the National Health & Medical Research Council (NHMRC) of Australia, a project grant (grant reference number 11-0563) from the Association for

International Cancer Research (AICR), and an Establishment Grant (ref. 2831/2009) to C.V.H. from the Clive and Vera Ramaciotti Foundation. A.J.T. is supported by The Wellcome Trust and the National Institute for Health Research Biomedical Research Centre at Great Ormond Street Hospital for Children NHS Foundation Trust and University College London. E.T.T. is supported by The Kids Cancer Alliance. We thank Dr. Ben Roediger (Immune Imaging Program, Centenary Institute, Camperdown, NSW, Australia) for reading the manuscript.

REFERENCES

1. Cavazzana-Calvo, M., Hacein-Bey, S., de Saint Basile, G., Gross, F., Yvon, E., Nusbaum, P., Selz, F., Hue, C., Certain, S., Casanova, J.L., et al. (2000). Gene therapy of human severe combined immunodeficiency (SCID)-X1 disease. Science *288*, 669–672.
2. Gaspar, H.B., Parsley, K.L., Howe, S., King, D., Gilmour, K.C., Sinclair, J., Brouns, G., Schmidt, M., Von Kalle, C., Barington, T., et al. (2004). Gene therapy of X-linked severe combined immunodeficiency by use of a pseudotyped gammaretroviral vector. Lancet *364*, 2181–2187.
3. Hacein-Bey-Abina, S., Garrigue, A., Wang, G.P., Soulier, J., Lim, A., Morillon, E., Clappier, E., Caccavelli, L., Delabesse, E., Beldjord, K., et al. (2008). Insertional oncogenesis in 4 patients after retrovirus-mediated gene therapy of SCID-X1. J. Clin. Invest. *118*, 3132–3142.
4. Howe, S.J., Mansour, M.R., Schwarzwaelder, K., Bartholomae, C., Hubank, M., Kempski, H., Brugman, M.H., Pike-Overzet, K., Chatters, S.J., de Ridder, D., et al. (2008). Insertional mutagenesis combined with acquired somatic mutations causes leukemogenesis following gene therapy of SCID-X1 patients. J. Clin. Invest. *118*, 3143–3150.
5. Ginn, S.L., Liao, S.H., Dane, A.P., Hu, M., Hyman, J., Finnie, J.W., Zheng, M., Cavazzana-Calvo, M., Alexander, S.I., Thrasher, A.J., and Alexander, I.E. (2010). Lymphomagenesis in SCID-X1 mice following lentivirus-mediated phenotype correction independent of insertional mutagenesis and gammac overexpression. Mol. Ther. *18*, 965–976.
6. Holyoake, T.L., Freshney, M.G., Samuel, K., Ansell, J., Watson, G.E., Wright, E.G., Graham, G.J., and Pragnell, I.B. (2001). In vivo expansion of the endogenous B-cell compartment stimulated by radiation and serial bone marrow transplantation induces B-cell leukaemia in mice. Br. J. Haematol. *114*, 49–56.
7. Martins, V.C., Ruggiero, E., Schlenner, S.M., Madan, V., Schmidt, M., Fink, P.J., von Kalle, C., and Rodewald, H.R. (2012). Thymus-autonomous T cell development in the absence of progenitor import. J. Exp. Med. *209*, 1409–1417.
8. Peaudecerf, L., Lemos, S., Galgano, A., Krenn, G., Vasseur, F., Di Santo, J.P., Ezine, S., and Rocha, B. (2012). Thymocytes may persist and differentiate without any input from bone marrow progenitors. J. Exp. Med. *209*, 1401–1408.
9. Boehm, T. (2012). Self-renewal of thymocytes in the absence of competitive precursor replenishment. J. Exp. Med. *209*, 1397–1400.
10. Martins, V.C., Busch, K., Juraeva, D., Blum, C., Ludwig, C., Rasche, V., Lasitschka, F., Mastitsky, S.E., Brors, B., Hielscher, T., et al. (2014). Cell competition is a tumour suppressor mechanism in the thymus. Nature *509*, 465–470.
11. McCormack, M.P., Young, L.F., Vasudevan, S., de Graaf, C.A., Codrington, R., Rabbitts, T.H., Jane, S.M., and Curtis, D.J. (2010). The *Lmo2* oncogene initiates leukemia in mice by inducing thymocyte self-renewal. Science *327*, 879–883.
12. Lo, M., Bloom, M.L., Imada, K., Berg, M., Bollenbacher, J.M., Bloom, E.T., Kelsall, B.L., and Leonard, W.J. (1999). Restoration of lymphoid populations in a murine model of X-linked severe combined immunodeficiency by a gene-therapy approach. Blood *94*, 3027–3036.
13. Vicente, R., Adjali, O., Jacquet, C., Zimmermann, V.S., and Taylor, N. (2010). Intrathymic transplantation of bone marrow-derived progenitors provides long-term thymopoiesis. Blood *115*, 1913–1920.
14. Almeida, A.R., Borghans, J.A., and Freitas, A.A. (2001). T cell homeostasis: Thymus regeneration and peripheral T cell restoration in mice with a reduced fraction of competent precursors. J. Exp. Med. *194*, 591–599.
15. Thomas-Vaslin, V., Altes, H.K., de Boer, R.J., and Klatzmann, D. (2008). Comprehensive assessment and mathematical modeling of T cell population dynamics and homeostasis. J. Immunol. *180*, 2240–2250.
16. Tuckett, A.Z., Thornton, R.H., Shono, Y., Smith, O.M., Levy, E.R., Kreines, F.M., van den Brink, M.R., and Zakrzewski, J.L. (2014). Image-guided intrathymic injection of multipotent stem cells supports lifelong T-cell immunity and facilitates targeted immunotherapy. Blood *123*, 2797–2805.
17. Leroi, A.M., Koufopanou, V., and Burt, A. (2003). Cancer selection. Nat. Rev. Cancer *3*, 226–231.
18. Qasim, W., Gaspar, H.B., and Thrasher, A.J. (2014). "Darwinian" tumor-suppression model unsupported in clinical experience. Mol. Ther. *22*, 1562–1563.
19. Stein, S., Ott, M.G., Schultze-Strasser, S., Jauch, A., Burwinkel, B., Kinner, A., Schmidt, M., Krämer, A., Schwäble, J., Glimm, H., et al. (2010). Genomic instability and myelodysplasia with monosomy 7 consequent to EVI1 activation after gene therapy for chronic granulomatous disease. Nat. Med. *16*, 198–204.
20. Braun, C.J., Boztug, K., Paruzynski, A., Witzel, M., Schwarzer, A., Rothe, M., Modlich, U., Beier, R., Göhring, G., Steinemann, D., et al. (2014). Gene therapy for Wiskott-Aldrich syndrome–long-term efficacy and genotoxicity. Sci. Transl. Med. *6*, 227ra33.
21. Woods, N.B., Bottero, V., Schmidt, M., von Kalle, C., and Verma, I.M. (2006). Gene therapy: Therapeutic gene causing lymphoma. Nature *440*, 1123.
22. Scobie, L., Hector, R.D., Grant, L., Bell, M., Nielsen, A.A., Meikle, S., Philbey, A., Thrasher, A.J., Cameron, E.R., Blyth, K., and Neil, J.C. (2009). A novel model of SCID-X1 reconstitution reveals predisposition to retrovirus-induced lymphoma but no evidence of gammaC gene oncogenicity. Mol. Ther. *17*, 1031–1038.
23. Aiuti, A., Cassani, B., Andolfi, G., Mirolo, M., Biasco, L., Recchia, A., Urbinati, F., Valacca, C., Scaramuzza, S., Aker, M., et al. (2007). Multilineage hematopoietic reconstitution without clonal selection in ADA-SCID patients treated with stem cell gene therapy. J. Clin. Invest. *117*, 2233–2240.
24. Wiekmeijer, A.S., Pike-Overzet, K., IJSpeert, H., Brugman, M.H., Wolvers-Tettero, I.L., Lankester, A.C., Bredius, R.G., van Dongen, J.J., Fibbe, W.E., Langerak, A.W., et al. (2016). Identification of checkpoints in human t-cell development using severe combined immunodeficiency stem cells. J. Allergy Clin. Immunol. *137*, 517–526.
25. Ruggero, K., Al-Assar, O., Chambers, J.S., Codrington, R., Brend, T., and Rabbitts, T.H. (2016). LMO2 and IL2RG synergize in thymocytes to mimic the evolution of SCID-X1 gene therapy-associated T-cell leukaemia. Leukemia *30*, 1959–1962.
26. Demeocq, F., Viallard, J.L., Boumsell, L., Richard, Y., Chassagne, J., Plagne, R., Lemerle, J., and Bernard, A. (1982). The correlation of adenosine deaminase and purine nucleoside phosphorylase activities in human lymphocytes subpopulations and in various lymphoid malignancies. Leuk. Res. *6*, 211–220.
27. Tarantal, A.F., Giannoni, F., Lee, C.C., Wherley, J., Sumiyoshi, T., Martinez, M., Kahl, C.A., Elashoff, D., Louie, S.G., and Kohn, D.B. (2012). Nonmyeloablative conditioning regimen to increase engraftment of gene-modified hematopoietic stem cells in young rhesus monkeys. Mol. Ther. *20*, 1033–1045.
28. Park, J.Y., Kob, M., Prodeus, A.P., Rosen, F.S., Shcherbina, A., and Remold-O'Donnell, E. (2004). Early deficit of lymphocytes in Wiskott-Aldrich syndrome: Possible role of WASP in human lymphocyte maturation. Clin. Exp. Immunol. *136*, 104–110.
29. Cotta-de-Almeida, V., Westerberg, L., Maillard, M.H., Onaldi, D., Wachtel, H., Meelu, P., Chung, U.I., Xavier, R., Alt, F.W., and Snapper, S.B. (2007). Wiskott Aldrich syndrome protein (WASP) and N-WASP are critical for T cell development. Proc. Natl. Acad. Sci. USA *104*, 15424–15429.
30. Zhang, J., Shehabeldin, A., da Cruz, L.A., Butler, J., Somani, A.K., McGavin, M., Kozieradzki, I., dos Santos, A.O., Nagy, A., Grinstein, S., et al. (1999). Antigen receptor-induced activation and cytoskeletal rearrangement are impaired in Wiskott-Aldrich syndrome protein-deficient lymphocytes. J. Exp. Med. *190*, 1329–1342.
31. Karlsson, A., Ungerbäck, J., Rasmussen, A., French, J.E., and Söderkvist, P. (2008). Notch1 is a frequent mutational target in chemically induced lymphoma in mouse. Int. J. Cancer *123*, 2720–2724.
32. O'Neil, J., Calvo, J., McKenna, K., Krishnamoorthy, V., Aster, J.C., Bassing, C.H., Alt, F.W., Kelliher, M., and Look, A.T. (2006). Activating Notch1 mutations in mouse models of T-ALL. Blood *107*, 781–785.

33. Onozawa, M., and Aplan, P.D. (2012). Illegitimate V(D)J recombination involving nonantigen receptor loci in lymphoid malignancy. Genes Chromosomes Cancer *51*, 525–535.

34. Pear, W.S., and Aster, J.C. (2004). T cell acute lymphoblastic leukemia/lymphoma: A human cancer commonly associated with aberrant NOTCH1 signaling. Curr. Opin. Hematol. *11*, 426–433.

35. Tsuji, H., Ishii-Ohba, H., Noda, Y., Kubo, E., Furuse, T., and Tatsumi, K. (2009). Rag-dependent and Rag-independent mechanisms of Notch1 rearrangement in thymic lymphomas of *Atm*(-/-) and scid mice. Mutat. Res. *660*, 22–32.

36. Tsuji, H., Ishii-Ohba, H., Katsube, T., Ukai, H., Aizawa, S., Doi, M., Hioki, K., and Ogiu, T. (2004). Involvement of illegitimate V(D)J recombination or microhomology-mediated nonhomologous end-joining in the formation of intragenic deletions of the Notch1 gene in mouse thymic lymphomas. Cancer Res. *64*, 8882–8890.

37. Tsuji, H., Ishii-Ohba, H., Ukai, H., Katsube, T., and Ogiu, T. (2003). Radiation-induced deletions in the 5′ end region of Notch1 lead to the formation of truncated proteins and are involved in the development of mouse thymic lymphomas. Carcinogenesis *24*, 1257–1268.

38. Hu, M., Watson, D., Zhang, G.Y., Graf, N., Wang, Y.M., Sartor, M., Howden, B., Fletcher, J., and Alexander, S.I. (2008). Long-term cardiac allograft survival across an MHC mismatch after "pruning" of alloreactive CD4 T cells. J. Immunol. *180*, 6593–6603.

39. Walters, G., and Alexander, S.I. (2004). T cell receptor BV repertoires using real time PCR: A comparison of SYBR green and a dual-labelled HuTrec fluorescent probe. J. Immunol. Methods *294*, 43–52.

40. Sempowski, G.D., and Rhein, M.E. (2004). Measurement of mouse T cell receptor excision circles. Curr. Protoc. Immunol. *Chapter 10*. Unit 10 31.

41. Broers, A.E., Meijerink, J.P., van Dongen, J.J., Posthumus, S.J., Löwenberg, B., Braakman, E., and Cornelissen, J.J. (2002). Quantification of newly developed T cells in mice by real-time quantitative PCR of T-cell receptor rearrangement excision circles. Exp. Hematol. *30*, 745–750.

42. Li, H., and Durbin, R. (2009). Fast and accurate short read alignment with Burrows-Wheeler transform. Bioinformatics *25*, 1754–1760.

43. Koboldt, D.C., Chen, K., Wylie, T., Larson, D.E., McLellan, M.D., Mardis, E.R., Weinstock, G.M., Wilson, R.K., and Ding, L. (2009). VarScan: Variant detection in massively parallel sequencing of individual and pooled samples. Bioinformatics *25*, 2283–2285.

44. Li, H., Handsaker, B., Wysoker, A., Fennell, T., Ruan, J., Homer, N., Marth, G., Abecasis, G., and Durbin, R.; 1000 Genome Project Data Processing Subgroup (2009). The Sequence Alignment/Map format and SAMtools. Bioinformatics *25*, 2078–2079.

45. Wang, J., Mullighan, C.G., Easton, J., Roberts, S., Heatley, S.L., Ma, J., Rusch, M.C., Chen, K., Harris, C.C., Ding, L., et al. (2011). CREST maps somatic structural variation in cancer genomes with base-pair resolution. Nat. Methods *8*, 652–654.

46. Wang, K., Li, M., and Hakonarson, H. (2010). ANNOVAR: Functional annotation of genetic variants from high-throughput sequencing data. Nucleic Acids Res. *38*, e164.

47. Robinson, J.T., Thorvaldsdóttir, H., Winckler, W., Guttman, M., Lander, E.S., Getz, G., and Mesirov, J.P. (2011). Integrative genomics viewer. Nat. Biotechnol. *29*, 24–26.

48. Irizarry, R.A., Hobbs, B., Collin, F., Beazer-Barclay, Y.D., Antonellis, K.J., Scherf, U., and Speed, T.P. (2003). Exploration, normalization, and summaries of high density oligonucleotide array probe level data. Biostatistics *4*, 249–264.

49. Gentleman, R.C., Carey, V.J., Bates, D.M., Bolstad, B., Dettling, M., Dudoit, S., Ellis, B., Gautier, L., Ge, Y., Gentry, J., et al. (2004). Bioconductor: Open software development for computational biology and bioinformatics. Genome Biol. *5*, R80.

50. Smyth, G.K. (2004). Linear models and empirical bayes methods for assessing differential expression in microarray experiments. Stat. Appl. Genet. Mol. Biol. *3*, Article3.

51. Benjamini, Y., and Hochberg, Y. (1995). Controlling the false discovery rate: A practical and powerful approach to multiple testing. J. R. Stat. Soc. B *57*, 289–300.

52. Cullion, K., Draheim, K.M., Hermance, N., Tammam, J., Sharma, V.M., Ware, C., Nikov, G., Krishnamoorthy, V., Majumder, P.K., and Kelliher, M.A. (2009). Targeting the Notch1 and mTOR pathways in a mouse T-ALL model. Blood *113*, 6172–6181.

53. Ramsden, D.A., McBlane, J.F., van Gent, D.C., and Gellert, M. (1996). Distinct DNA sequence and structure requirements for the two steps of V(D)J recombination signal cleavage. EMBO J. *15*, 3197–3206.